Casimir Effect for spherical boundaries: A thermofield dynamics approach

D.U. Matrasulov[*], Kh.T. Butanov[*], Kh.Yu. Rakhimov[*]
F.C. Khanna[†], and A.E. Santana[‡]

Abstract

The Casimir effect for spherical geometry is calculated using generalized Thermofield Dynamics for the case of scalar field. Casimir force and Casimir pressure are presented. It is found that for high temperatures the Casimir force does change sign.

1 Introduction

Casimir effect and its applications have been a topic of extensive experimental and theoretical studies since its first prediction in 1948 [1]-[9]. It has been measured in experiments [2]-[5] involving spherical metallic and non-mettalic balls [5] and has thus led to its application as switching mechanism in nano-technology. Role of finite temperature on the Casimir effect has been considered theoretically [5]-[8] but, in general, the magnitude of the force is too small to be measured precisely. Recently Casimir-Polder force, along with the effect of finite temperature, has been measured between a bulk object and a gas-phase atom [10]. Effect of finite temperature on Casimir effect, force between two bulk such as two metallic objects or two dielectric objects, has eluded detection due to the fact that the variation with temperature is very small. However it is becoming important to calculate the Casimir force in a spherical geometry that involves particles. Such is the case of baryons, in particle physics, that have quark confinement and it is expected that the quarks deconfine at high temperature. This is the central objective at facilities such as RHIC, that allows collisions between heavy ion beams, and LHC, that will allow collisions between heavy ion beams like Pb at much higher energies. The object is to de-confine the quarks and thus form a quark-gluon plasma, a form of matter that is believed to have existed soon after the big bang. The cosmology suggests that, the free quarks and gluons, as they cool down, combine into a confined state that are the baryons that eventually lead to the formation of nuclei at a later epoch of the universe. This suggests that the Casimir energy, in particular at finite temperature, would play an important role in the confinement and then the de-confinement of quarks and gluons. However we know that the dynamics of quarks and gluons is based on a non-Abelian theory of strong interactions, Quantum Chromo-Dynamics(QCD). Such a theory presents its own sort of difficulties due its non-Abelian nature. In this paper we will study the case of spherical geometry of the confined

---
[*]Heat Physics Department of the Uzbek Academy of Sciences, 28 Katartal St., 700135 Tashkent, Uzbekistan
[†]Physics Department University of Alberta Edmonton Alberta, T6G 2J1 Canada and TRIUMF, 4004 Wersbrook Mall, Vancouver, British Columbia, Canada, V6T2A3
[‡]Instituto de Física, Universidade de Brasília, 70910-900, Brasília-DF, Brazil

system but with an Abelian theory, in particular, for a scalar field. Studies with QCD will be considered separately. The present study uses the techniques developed recently and are based on using thermofield dynamics (TFD), real time finite temperature field theory, to get the finite temperature effects. This approach depends on using the Bogoliubov transformation to include the temperature in quantum field theory [13, 14, 15]. It is well-known that finite temperature Green's functions obey KMS condition that obeys periodicity (for Bosons) or anti-periodicity (Fermions) condition in temperature. This may be viewed as a confinement condition with temperature [16]-[18]. This has been extended with a great deal of success to the study of Casimir effect in a box or a paralellopiped. This technique will be used first for zero temperature case and then the spherical geometry. Then the Casimir effect may be interpreted as a vacuum condensation of the field in a confined geometry. Such an interpretation follows the original work that gave an elegant understanding of Superconductivity. The study will focus on calculating the Casimir energy and Casimir force for a field confined in a spherical geometry when the role of finite varying temperature is included. The study is based on the earlier work of Bender and Hays [21] to finite temperature using the techniques mentioned above. Additional work at zero temperature has been carried by several authors [19]-[26]. It is important to note that our technique will allow a variation with size of the spherical bag and with temperature quite easy. In section 2, necessary details of TFD will be presented. Section 3 gives details of the Casimir effect at $T = 0$. In section 4, application of TFD to the calculation of the Casimir effect at finite temperature will be provided. In section 5, numerical results and their comparison to earlier calculations will be shown. Variations with T and size of the sphere will be displayed. Finally some concluding remarks and future directions will be presented.

2   Generalization of TFD

The idea of compactification is based on the Bogoliubov transformations (BT). Briefly the idea is the following: The Green's function according to TFD prescription is given by a 2×2 matrix with the elements

$$G^{11} = G_0 + v^2(\omega, \beta)[G_0 - G_0^*], \tag{1}$$

$$G^{22} = -G_0^* + v^2(\omega, \beta)[G_0 - G_0^*],$$

$$G^{12} = G^{21} = v(\omega, \beta)[1 + v^2(\omega, \beta)]^{1/2}[G_0 - G_0^*]$$

with

$$v^2(\omega, \beta) = \frac{1}{e^{\beta|\omega|} - 1}.$$

The physically observable quantities are related to G^{11} only [13].

The finite-temperature Green's function in TFD is expressed in terms of the zero-temperature one using the Bogoliubov transformations which are defined as (for the case of bosons)

$$v^2(\omega, \beta) = \frac{1}{e^{\beta\omega} - 1} = \sum_{l=1}^{\infty} e^{-l\beta\omega}. \tag{2}$$

The finite-temperature Green's function in the momentum representation is expressed via the zero-temperature one as follows (here we write only $11-$element of the 2×2-matrix, while other elements can be obtained similarly):

$$G^{k,\beta} = G_0(k) + v^2(k, \beta)[G_0(k) + \tilde{G}_0(k)] \tag{3}$$

which defines the Green's function in the coordinate representation as

$$G^{11}(x - x', \beta) = \frac{1}{(2\pi)^2} \int d^4q \, G^{11}(q, \beta) e^{iq(x-x')} = G^{11}(\vec{x} - \vec{x}', x_0 - i\beta) \tag{4}$$

where q and x are four-vectors.

These transformations can be generalized by introducing the factor

$$v^2(q, \alpha) = \sum_{l=1}^{\infty} e^{-i\alpha_l q} \tag{5}$$

where the notation

$$\sum_{l=1}^{\infty} e^{-i\alpha_l \cdot q} = \sum_{l_0,l_1,l_2,l_3=1}^{\infty} exp[-i(\alpha_0 l_0 q_0 + \alpha_1 l_1 q_1 + \alpha_2 l_2 q_2 + \alpha_3 l_3 q_3)] \tag{6}$$

is used.

Then the Green's function obtained by applying the Bogoliubov transformation is written as

$$G^{11}(x - x', \alpha) = \frac{1}{(2\pi)^4} \int d^4q \, G^{11}(q, \alpha) e^{iq(x-x')} =$$
$$\frac{1}{(2\pi)^4} \int d^4q \, e^{iq(x-x')} \sum_{l=1}^{\infty} e^{-i\alpha_l \cdot q} [G_0^{11}(q) + \tilde{G}_0^{11}(q)] =$$
$$2 \sum_{l=1}^{\infty} G^{11}(x - x' - \alpha_l). \tag{7}$$

Thus the finite-temperature Green's function within the generalized TFD prescription is obtained from the zero-temperature Green's function using the Bogoliubov transformation. In section 4 we will use this Green's function to calculate the Casimir energy at finite temperature.

3   Casimir energy for spherical boundaries

The Casimir energy for spherical boundaries is explored in several approaches and by many authors (for review see [6]). In this section we give a brief description of the derivation of the Casimir energy based on the Green's function approach following Bender and Hays [21]. In the Green's function based approach the Casimir energy is calculated as [6, 21]

$$E_C = \lim_{\tau \to 0} \frac{\partial^2}{\partial \tau^2} \int d^3x \, \Gamma(\vec{x}, \vec{x}, \tau) \tag{8}$$

where $\Gamma(\vec{x}, \vec{x}, \tau)$ is the inhomogeneous part of the Green's function which is given by

$$G(\vec{x}, \vec{x}', x - x_0) = G_0(x - x') + \Gamma(\vec{x}, \vec{x}, x - x_0).$$

For the spherical boundaries the (Fourier transformed) Green's function is given by (for Dirichlet boundary conditions)

$$G(\vec{x}, \vec{x}', \omega) = ik \sum_{l=0}^{\infty} \left[j_l(kr') h_l^{(1)}(kr) - \frac{h_l^{(1)}(kR)}{j_l(kR)} j_l(kr') j_l(kr) \right] \sum_{m=-l}^{l} Y_{lm}(\Omega) Y_{lm}(\Omega') \tag{9}$$

where $h_l^{(1)}(x)$ is the Hankel function of the first order, $j_l(kr)$ is the spherical Bessel function, $k = |\omega|$ and R is radius of the sphere. Second term in this expression is the inhomogeneous part of the Green's function:

$$\Gamma(\vec{x}, \vec{x}', \omega) = -ik \sum_{l=0}^{\infty} \left[\frac{h_l^{(1)}(kR)}{j_l(kR)} j_l(kr') j_l(kr) \right] \sum_{m=-l}^{l} Y_{lm}(\Omega) Y_{lm}(\Omega'). \tag{10}$$

Then the Casimir energy is written as

$$E(R, \tau) = \sum_{l=0}^{\infty} (2l+1) \frac{\partial^2}{\partial \tau^2} \int_{-\infty}^{\infty} \frac{d\omega}{2\pi} e^{-i\omega\tau} k \frac{h_l^{(1)}(kR)}{j_l(kR)} \int_0^R dr\, r^2 j_l^2(kr) \tag{11}$$

where the orthogonality relation

$$\sum_{m=-l}^{l} Y_{lm}^2(\Omega) = \frac{2l+1}{4\pi}$$

is used.

The radial integral can be expressed in terms of Bessel functions:

$$\int_0^R dr\, r^2 j_l^2(kr) = \frac{R^2}{2} [j_l^2(kR) - j_{l-1}(kR) j_{l+1}(kR)]$$

which allows us to write eq. (11) as

$$E(R, \tau) = -\frac{1}{2} \sum_{l=0}^{\infty} (2l+1) \int_{-\infty}^{\infty} \frac{d\omega}{2\pi} e^{-i\omega\tau} i(kR)^3 \frac{h_l^{(1)}(kR)}{j_l(kR)} [j_l^2(kR) - j_{l-1}(kR) j_{l+1}(kR)]. \tag{12}$$

Using the Wick rotations

$$\omega \to i\omega, \quad \tau \to i\tau, \quad k \to i|\omega|$$

and the substitutions

$$x = |\omega| R, \quad \delta = \tau/R$$

this expression is written in the form

$$E(R, \tau) = \lim_{\delta \to 0} \frac{1}{2\pi R} \sum_{l=0}^{\infty} (2l+1) \int_0^{\infty} dx\, x^2 \cos(\delta x) \frac{K_{l+1/2}(x)}{I_{l+1/2}(x)} [I_{l+1/2}^2(x) - I_{l-1/2}(x) I_{l+3/2}(x)].$$

In this expression the integral does not contain $R-$ dependance. Therefore the Casimir energy is proportional to R^{-1}.

4 Calculation at finite temperature

Now we consider the Casimir effect at finite temperature. The generalised TFD formalism is used when the field is coupled to a heat bath. The above discussed generalized thermofield dynamics formalism can be used in this case to calculate the zero-point energy at finite temperature. To do this we need to rewrite the generalized BT, which can be written in spherical coordinates.

Then the Green's function is written as

$$G(\vec{x}, \vec{x}', x - x_0) = \frac{1}{(2\pi)^4} \int d^3q \, dq_0 \, G(\vec{q}, q_0) e^{i\vec{q}(\vec{r}-\vec{r}')} e^{iq_0 x_0}. \tag{13}$$

With the prescription for the generalized BT, $G(\vec{q}, q_0)$ is written as

$$G(\vec{q}, q_0, \vec{\alpha}, \alpha_0) = \sum_{\vec{l}, l_0 = 1}^{\infty} e^{-i\vec{\alpha}_{\vec{l}} \vec{q}} e^{-iq_0 \alpha_{l_0}} G(\vec{q}, q_0) \tag{14}$$

where $\vec{l} = (l_r, l_\theta, l_\phi)$, $\vec{\alpha}_{\vec{l}} = (l_r \alpha_r, l_\theta \alpha_\theta, l_\phi \alpha_\phi)$ and $\alpha_{l_0} = l_0 \alpha_0$

$$G(\vec{x}, \vec{x}', x - x_0, \vec{\alpha}, \alpha_0) = \frac{1}{(2\pi)^4} \int d^3q \, dq_0 \, e^{i\vec{q}(\vec{r}-\vec{r}')} e^{iq_0 x_0} \sum_{\vec{l}, l_0 = 1}^{\infty} e^{-i\vec{\alpha}_{\vec{l}} \vec{q}} e^{i\alpha_{l_0} q_0} G_0(\vec{q}, q_0) =$$

$$\frac{1}{(2\pi)^4} \sum_{\vec{l}, l_0 = 1}^{\infty} \int d^3q \, dq_0 \, e^{i\vec{q}(\vec{r}-\vec{r}'-\vec{\alpha}_{\vec{l}})} e^{iq_0(x_0 - \alpha_{l_0})} G_0(\vec{q}, q_0). \tag{15}$$

Denoting $\vec{r}'' = \vec{r}' - \vec{\alpha}_{\vec{l}}$ we have

$$G(\vec{x}, \vec{x}', x - x_0, \vec{\alpha}, \alpha_0) = \frac{1}{(2\pi)^4} \sum_{\vec{l}, l_0 = 1}^{\infty} \int d^3q \, dq_0 \, e^{i\vec{q}(\vec{r}-\vec{r}'')} e^{iq_0(x_0 - \alpha_{l_0})} G_0(\vec{q}, q_0) \equiv G(\vec{r}, \vec{r}'', x_0 - \alpha_{l_0}) \tag{16}$$

Then for the compactified finite-temperature Green's function for spherical boundries (for Boson case) is given as

$$G(\vec{x}, \vec{x}', \alpha) = ik_1 \sum_{l=0}^{\infty} \sum_{\vec{l}, l_0 = 1}^{\infty} [j_l(k_1 r'') h_l^1(k_1 r) - \frac{h_l^1(k_1 R)}{j_l(k_1 R)} j_l(k_1 r'') j_l(k_1 r)] \sum_{m=-l}^{l} Y_{lm}(\Omega') Y_{lm}(\Omega'') \tag{17}$$

where, $k_1 = |\omega - il_0 \alpha_0|$, Ω' is the angle between r and r'', $r'' = r' - l_r \alpha_r$. For the compactified Casimir energy we have from eq. (12)

$$E(R, \alpha) = \lim_{\tau \to -il_0 \alpha_0} \sum_{l_0, l_r = 1}^{\infty} \sum_{l=0}^{\infty} (2l + 1) \frac{\partial^2}{\partial \tau^2} \int_{-\infty}^{\infty} \frac{d\omega}{2\pi} e^{-i(\omega - il_0 \alpha_0)\tau} k_1 \frac{h_l^1(k_1 R)}{j_l(k_1 R)} L(R, k_1, \alpha_r) \tag{18}$$

where

$$L(R, k_1, \alpha_r) \equiv \int_0^R dr \, r^2 j_l(k_1 r) j_l(k_1(r - l_r \alpha_r)). \tag{19}$$

Unlike the case of zero-temperature, when $\alpha_0 = \alpha_r = 0$, R-dependence is not factorized in the case of finite temperature and thus this dependence cannot be written explicitly.

5 Results

The Casimir energy is calculated numerically for a sphere with radius a for several values of β and the compactification parameter, α_r. In the case of zero temperature calculations of the Casimir energy diverge due to the divergence of the integral for the Green's function over r (between limits from 0 to a). This divergence can be regularized by replacing upper integration limit by $a(1 - \epsilon)$ with *epsilon* $\to 1$. In the case of finite-temperature such a
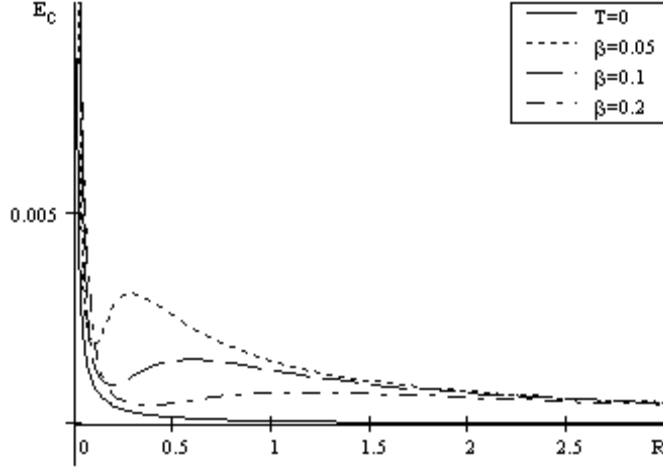
Figure 1: Dependences of the Casimir energy on the sphere radius at different temperatures and fixed α_r ($\alpha_r = 10^{-6}$) are compared with the corresponding zero-temperature result plotted from ref.[21].

divergence is suppressed due to the presence of the factor $e^{-l_0\alpha_0\tau}$ in eq. (18). In Fig. 1 Casimir energy is plotted as a function of the radius for different temperatures at the fixed value of $\alpha_r = 10^{-6}$ and compared with the Casimir energy at zero temperature.

The lowest curve in this figure shows the Casimir energy for $T = 0$ calculated on the basis of the approach developed by Bender and Hays (using ϵ-type cutoff). The following values of β are chosen: $\beta = 0.2$, $\beta = 0.1$ and $\beta = 0.05$. It is clear that, in certain interval of R, an increase of the temperature leads to considerable changes in the $E(R)$ and for higher enough values of T this curve has a maximum, which corresponds to a sign change of the Casimir pressure(derivative of the $E(R)$ over with R).
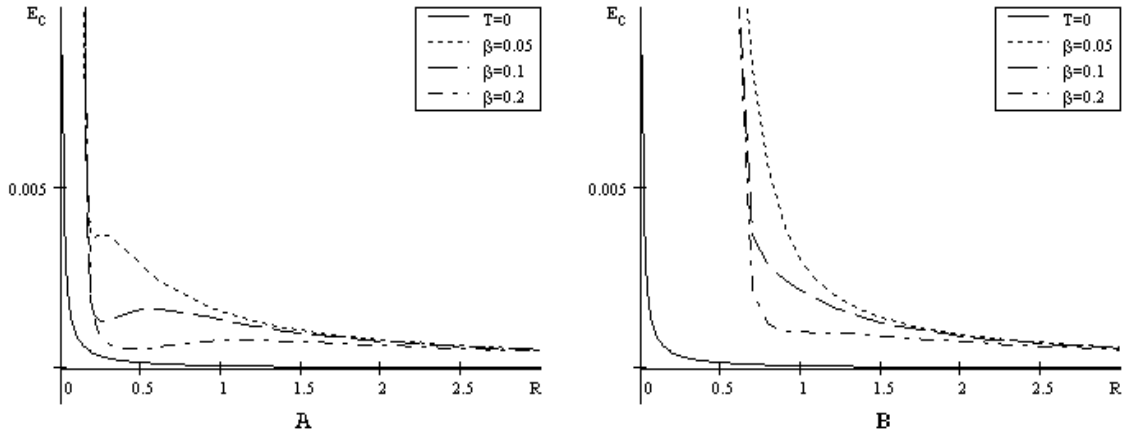

Figure 2: Dependence of the Casimir energy at different temperatures and for fixed α_r. A: for $\alpha_r = 0.1$; B: $\alpha_r = 0.5$.

However, the situation changes for larger values of α_r. As shown in Fig. 2, for higher values of α_r these maxima and minima disappear and the difference (distance) between the finite temperature and $T = 0$ curves increase. In other words, increasing (α_r) leads to the suppression of the extremum points in the $E(R)$-curve.

This can be understood if results in Fig. 3, where the integral L is plotted as a function of R for different values of α_r are considered. It is clear in this plot that by increasing α_r the curve shifts from right to left side i.e. the compactification parameter is higher as the $L(R)$-curve is closer to the vertical axis. As the only difference in $E(R)$ for different values of α_r arises from the integral $L(R, \alpha_r)$ the difference between various $E(R)$ corresponding to different values of α_r is similar to that for $L(R)$ at various α_r. The comparison of the
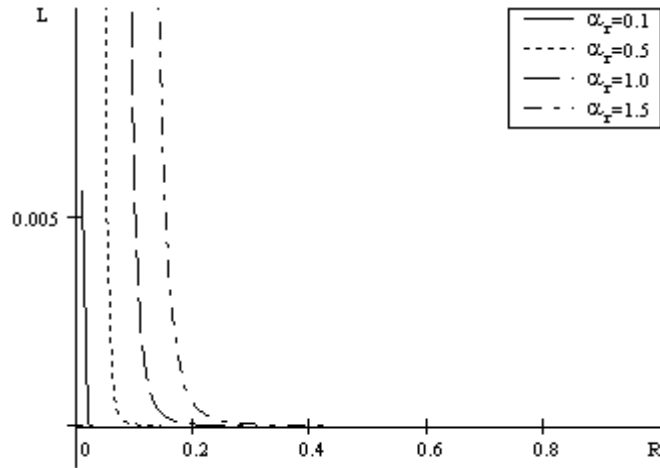

Figure 3: The quantity $L(R)$ for different values of $\alpha_r = 0.1$.

R-dependence of Casimir energy for $\beta = 1.2$, $\beta = 1.5$ ($\alpha_r = 0$) and $T = 0$ (from [21]) in Fig. 4 shows that our results approach those obtained by Bender and Hays, as temperature approaches zero. In Fig. 5 plots for the Casimir pressure for various values of β are presented. Three values of temperature are considered in this case, $\beta = 0.2$, $\beta = 0.1$ and $\beta = 0.05$ for $\alpha_r = 10^{-6}$ and $\alpha_r = 0.1$. It is clear from these plots that at certain values of R corresponding to maxima and minima of the curve $E(R)$ the function $P(R)$ changes its sign one or two times depending on the value of β. Therefore one may consider the critical temperature where the Casimir pressure becomes negative. This critical temperature depends on the radius of the sphere, i.e. for different values of R we get different values of the critical temperature. In addition, it depends on the value of the compactification parameter, α_r whose increase leads to making a "smooth" $E(R)$ curve and the maxima and minima in this curve are suppressed. In other words, in the R-dependence of the Casimir energy, the increase of α_r plays a similar role as that of increasing β, i.e., decreasing of T.

6   Conclusions

Thus we have treated Casimir effect for spherical boundaries at finite temperature using the prescription of generalized thermofield dynamics. Within this approach the heat bath effects
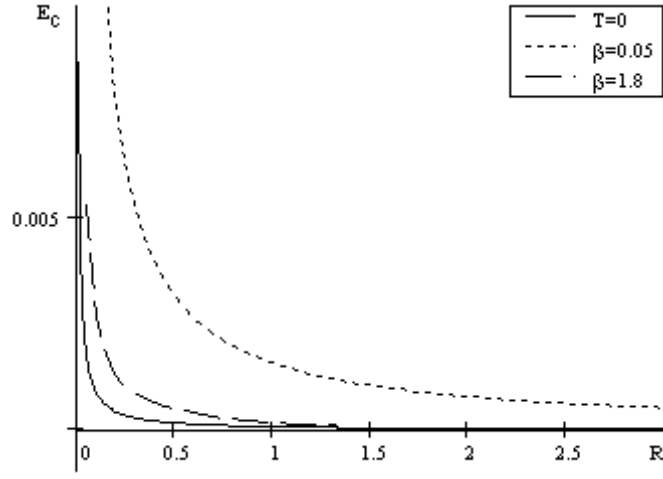
Figure 4: Casimir energy as a function of R for different temperatures at $\alpha_r = 0$.
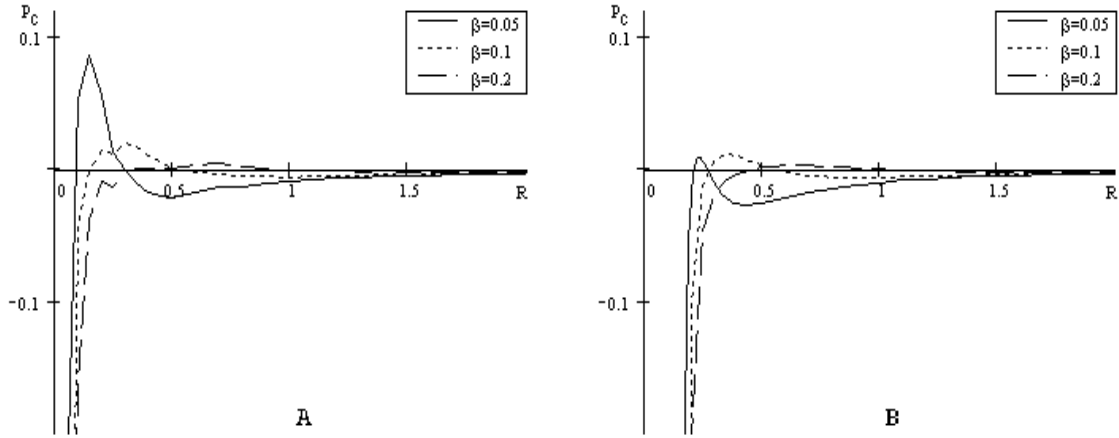

Figure 5: Dependence of the Casimir pressure on the sphere radius for different temperatures and fixed α_r. A: for $\alpha_r = 10^{-6}$; B: $\alpha_r = 0.1$.

and space compactification effects (which means the presence of the spatial periodicity) in the zero-point energy and Casimir pressure are studied. The results show that the dependence of the Casimir energy on the spherical radius is considerably different than that in the case of zero temperature results obtained by Bender and Hays and others. The first difference is the fact that, unlike the case of the zero temperature, the R-dependence of the Casimir energy is not factorized in the case of $T \neq 0$. This leads to other differences between finite and zero temperature results. In particular as temperature decreases the form of $E(R)$-curve changes and for higher values of temperature maxima and minima can appear in this curve. This implies a change of the sign for the Casimir pressure. However, such changes can be suppressed by increasing (α_r) and, in addition, these extremum points can be suppressed and curve becomes smooth. We note that the heat bath effects become considerable for rather small values of β. It is clear from Fig. 3 that the difference between zero-temperature and finite temperature Casimir energies disappears for values of β higher than 1.5. Therefore the "convenient" candidate system where finite temperature effects can be found should be considered among systems coupled to a strongly interacting environment, such as hadrons in quark-gluon plasma. This would imply that the magnitude of the de-confining temperature may be affected by the Casimir energy. Finally it is important to emphasize that the use of generalised Bogoliubov transformations provides a different perspective to the presence of Casimir energy i.e. it is a manifestation of condensation of the scalar field in the vacuum. It may be anticipated that for a real nucleon with quarks and gluons as its content in a spherical surroundings, the Casimir energy may be viewed as a condensation of quark and gluon fields in the vacuum. These considerations make a study of a real nucleon with QCD field involving quarks and gluons a rather fascinating subject to explore. Such a study is presently in progress.

Acknowledgements

References

[1] H.B.G. Casimir, Proc. Kon. Ned. Akad. **51**(1948) 793.

[2] B.V. Deriagin and I.I. Abrikosova, Sov. Phys. JEPT **3** (1957) 819.

[3] M.J. Sparnaay, Physica **24** (1958) 751.

[4] E.S. Sabisky and C.H. Anderson, Phys. Rev. A **7** (1973) 790.

[5] M. Bordag, U. Mohideen, V.M. Mostepanenko, Phys. Rep. **353** (2001) 1.

[6] G. Plunien, B. Muller and W. Greiner, Phys. Rep. **134** (1986) 87.

[7] V.M. Mostepanenko and N.N. Trunov,*Casimir Effect and its Applications.* (Oxford Science Publications, Oxford, 1997).

[8] K.A. Milton *The Casimir Effect* (World Scientific, Singapore, 2001).

[9] Steven K. Lamoreaux, Rep. Progr. Phys. **68** (2005) 201.

[10] J.M. Obrecht et.al., Phys. Rev. Lett. **98** (2007) 063201.

[11] C.D. Fosco and L.E. Oxman, Phys.Rev. D **75** (2007) 025029.

[12] A.R. Moura, A.R. Pereria and A.S.T. Pires, Phys. Rev. B **75** (2007) 014431.

[13] J.C. da Silva, F.C. Khanna, A. Matos Neto and A.E. Santana, Phys. Rev. A **66** 052101 (2002).

[14] H. Queiroz, J.C. da Silva, F.C. Khanna, J.M.C. Malboisson, M. Revzen, A.E. Santana, Ann. Phys. **317** (2005) 220.

[15] F.C. Khanna, J.M.C. Malbouisson and A.E. Santana *"Thermofield dynamics: Generalized Bogoliubov transformations and applications to Casimir effect"* F.C. Khanna and D.U. Matrasulov (eds.), Non-Linear Dynamics and Fundamental Interactions (2006) 215.

[16] H. Umezawa, H. Matsumoto and M. Tachiki *Thermofield Dynamics.* (North-Holland. Amsterdam, 1982).

[17] Y. Takahashi and H. Umezawa, Int. J. Mod. Phys. B **10** (1996) 1755.

[18] Ashok Das, *Finite Temperature Field Theory* (World Scientific, New York, 1977).

[19] T.H. Boyer, Phys. Rev. **174** (1968) 1764.

[20] B. Davies, J. Math. Phys. **13** (1971) 1324.

[21] Carl M. Bender and Patrick Hays, Phys. Rev. D **14** (1976) 2622.

[22] K.A. Milton, Phys. Rev. D **22** (1980) 1441.

[23] K.A. Milton, Phys. Rev. D **27** (1980) 439.

[24] M.E. Bowers and C.R. Hagen, Phys. Rev. D **59** (1999) 025007.

[25] C.R. Hagen, Phys. Rev. D **61** (2000) 065005.

[26] C.R. Hagen, Phys. Lett. A **300** (2002) 591.